

Design and Fabrication of a 4-DOF Industrial Robotic Arm

Mohamed Amr Sabry*, Youssef Khaled Mahran*,
Lina Tamer Ghonim*, Shaheer Sherif Shawky*, Mohammed Saeed* and Mariam Abdelrahman Fathi*

*German University in Cairo (GUC), Egypt

Emails: mohamedamramer@gmail.com ,youssef.mahran@student.guc.edu.eg , mohammed.saeed@student.guc.edu.eg,
lina.ghonim@student.guc.edu.eg, shaheer.aziz@student.guc.edu.eg, mariam.fathi@student.guc.edu.eg,

Keywords-Industrial Robotic Applications , robotic manipulators , DOF ,

I. INTRODUCTION

Industrial robotics is one of the fastest-growing fields in modern technology, enabling significant advances in automation, efficiency, and safety. Once limited to repetitive manufacturing tasks, robots are now entering industries that previously had limited automation, such as healthcare, food processing, and agriculture. This review explores recent advancements in industrial robotics, focusing on human-robot collaboration, object recognition, path planning, and optimization, as well as applications in the medical, agricultural, and food industries.

In robotic applications, time data processing allows these machines to achieve higher precision in tasks such as surgical procedures, food sorting, and crop harvesting. These innovations are driving a new era of automation, where robots are not only tools but integral partners in diverse industrial operations.

The scope of this review includes: Recent developments in human-machine interaction (HMI) and its increasing role in industries whether medical , food industry , assembly and material handling applications.

II. LITERATURE REVIEW

A. Human-machine Interaction (HMI)

Recent advancements in Human-Robot Collaboration (HRC) emphasize human-centered automation by integrating human activities with Cyber-Physical Production Systems (CPPS). This approach focuses on adapting industrial manipulators to the physiological characteristics of human operators, using biometric signals like stress, fatigue, and motion tracking. In a collaborative environment, a CPPS enables a robotic arm to assist a human operator in a joint manipulation task, where the robot adapts its task execution speed and operation based on real-time monitoring of the worker's condition. This ensures improved interaction and efficiency in the manufacturing process [1].

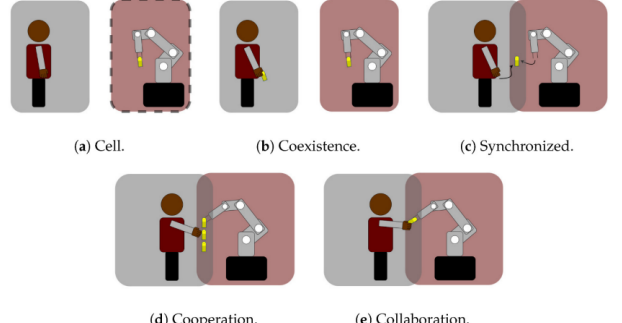


Fig. 1: Human–robot cooperation levels [5]: (a) no collaboration, the robot remains inside a closed work cell; (b) coexistence, removed cells, but separate workspaces; (c) synchronisation, sharing of the workspace, but never at the same time; (d) cooperation, shared task and workspace, no physical interaction; (e) collaboration, operators and robots exchange forces. [2]

B. Medical Applications

Serial robotic manipulators have revolutionized medical applications, particularly in surgery, by enhancing precision, dexterity, and reducing human error in complex procedures. One of the most prominent examples is the da Vinci Surgical System, which has been widely adopted for minimally invasive surgeries such as urology, gynecology, and cardiac operations. Yang et al. in 2024 addressed these systems, which utilize serial linkages to control end-effectors, enabling surgeons to perform tasks with enhanced precision and stability. In recent years, research has focused on improving the haptic feedback, control algorithms, and integration of machine learning (ML) for adaptive robotic behavior during surgery [3]. These manipulators are often structured with a series of revolute joints connected in a chain-like formation, enabling rotation around a fixed axis at each joint. This 7-DOF structure allows for intricate maneuvers such as rotation, pivoting, and precise angular adjustments, which are crucial in surgeries that require high precision in confined spaces, such as laparoscopic procedures [4].

C. Applications in Agriculture

The development of agricultural robots is gaining momentum to address labor shortages and rising food production

demands. Deploying multiple cooperating robots can reduce task duration, accomplish tasks impossible for a single robot, or enhance efficiency. This study [5] presents a cooperation strategy where two heterogeneous robots work together for grape harvesting: one robot (the expert) performs the harvesting, while the other (the helper) carries the harvested grapes. The cooperative methodology ensures safe and effective robot interactions. Field experiments validated the coordinated navigation algorithm and demonstrated the cooperative harvesting method, with recommendations for future improvements. The study also explores using logical, explainable decision-making based on mathematical lattice theory to enhance cooperation between autonomous robots in agricultural applications [5], [6].

In the field of agricultural robotics, end effectors designed for fruit harvesting are considered mechatronic subsystems. Their primary function is to individually detach fruit from stems and deposit them into temporary storage containers [7]. Robotic harvesting is a multifaceted process that integrates video cameras and recognition algorithms to identify ripe fruit, followed by gripping the fruit with a specialized gripper, moving it using a manipulator arm, and placing it in a designated storage area.

Yeshmukhametov et al. showcased in 2019 that harvesting grippers in agricultural applications can generally be categorized into two types. The first type includes precision grip end effectors, which are commonly employed for crops such as strawberries, apples, tomatoes, and sweet peppers (as discussed in [8]). The second type involves compression-based grippers, which feature larger contact areas between the fingers and offer limited or no capacity to transfer movement through the fingers. An example of these grippers is those that function by gripping and vibrating the trunks, as noted in [36].

D. Food Industry

As the global population grows, so does the demand for food, putting pressure on suppliers to improve efficiency and sustainability. Robotics and automation are seen as critical solutions in this sector, although the food industry has been slower to adopt these technologies compared to others. Robotics is being used in food production, packaging, and even cooking. With the development of robotic devices, such as soft grippers, handling delicate food items has become more efficient, reducing the risk of damage and contamination. In recent years, especially due to COVID-19, there has been a notable increase in automation and AI-enabled robotic applications in the restaurant industry, enhancing both food processing and service operations. [9] A study by Sanket et al. in 2022 [10] offers an in-depth evaluation of the use of robotics in the food processing industry, highlighting a relatively novel application area. The review emphasizes the transformative potential of robots in food handling, serving, palletizing, and packaging operations. Key considerations such as robot dynamics, economic efficiency, kinematics, human-robot interaction, hygiene, safety, and maintenance are discussed.

E. Assembly and Material Handling

Segura et al. [11] introduces and analyzes Context-Aware Cloud Robotics (CACR) for advanced material handling. Unlike the One-Time On-Demand Delivery (OTODD) method, CACR features context-aware services and effective load balancing. The paper outlines the system architecture, advantages, challenges, and applications of CACR. It also details key functions for material handling, such as decision-making mechanisms and cloud-enabled simultaneous localization and mapping. A case study demonstrates CACR's energy-efficient and cost-saving capabilities, with simulations confirming its superiority in improving energy efficiency and reducing costs in cognitive industrial IoT applications.

Another Four key structural components, in the following paper [12], were identified: interaction levels, work roles, communication interfaces, and safety control modes. The study found that physical contact-based collaboration, such as screwing assembly of small parts and handling heavyweight objects, is well-suited for the automotive industry. Additionally, certified augmented and virtual reality devices emerged as effective assistive technologies for safety and training needs. The categorization provided helps practitioners select compatible structural components that align with modern manufacturing requirements for highly personalized products.

A specific functionality is proposed by Blatnick et al. of the designed robotic manipulator which is the possibility of gripping of circular objects. [13]

III. MODEL PROPOSAL

In our selected industrial application, we propose designing a desktop 4-DOF serial manipulator system specifically for **cooperative pick-and-place tasks**. This setup will involve two manipulators working in tandem to demonstrate multi-robot cooperation by playing an **interactive X-O game**. The game not only makes the demonstration more engaging but also effectively showcases the concept of Multi-Robot Systems (MRS) Cooperation in a clear, tangible manner. By using the serial robotic manipulators to strategically place game pieces, this research illustrates how cooperative robots can work together to achieve common objectives, highlighting both their coordination and adaptability in industrial applications. By exploring the dynamics of robot cooperation in a controlled setting, we aim to lay the groundwork for practical implementations of multi-robot systems in real-world scenarios, driving innovation and improving operational workflows.

IV. LIST OF COMPONENTS

Part Name	Qty	Price Range (EGP)	Total Price (EGP)	Available / Place
Double Axis High-torque Servo Motors	4	550-760	2750-3800	Hand me downs / Future Electronics
Single Axis Servo Motor	1	-	-	-
Arduino	1	500-1500	500-1500	Personal/Future Electronics/RAM Electronics
Power Supply	1	150-300	150-300	-
Jumpers	Several	30-50	120	Maamoun/Future Electronics
Motor driver/servo shield (L293D)	1	100	100	RAM Electronics
3D Printed Parts	Several	1.5-3 EGP/gram	500-1500	-
Bearings	Several	10-30	-	-
Screws/Nuts/Bolts	Several	30	-	-

TABLE I: Components Summary

V. PROPOSED GRABCAD MODELS

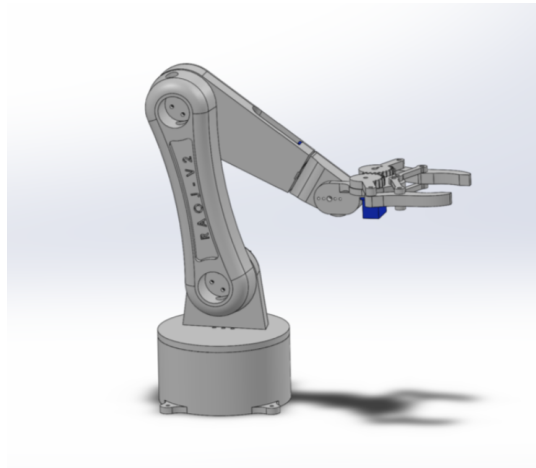


Fig. 2: Side view 1 of 4 DOF Proposed Robotic Arm

This is a gesture-controlled, 3D-printable, 5-degrees-of-freedom, desktop-sized robotic arm. The robotic arm is actuated using three standard servos and two micro servos. The arm is able to mimic human arm movements, which are detected using the Python OpenCV library. The PWM signals of the servos are processed in Python and sent to an Arduino Uno via serial. The links are short which decreases the dominance of the forces which will result in easier analysis and motors selection.

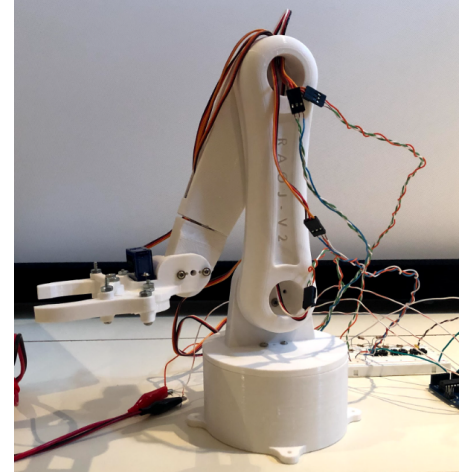


Fig. 3: Side view 2 of 4 DOF Proposed Robotic Arm

VI. FORWARD POSITION KINEMATICS

The forward position kinematics followed the Denavit–Hartenberg (DH) Convention. Firstly the robot frames were assigned as shown in Figure 4.

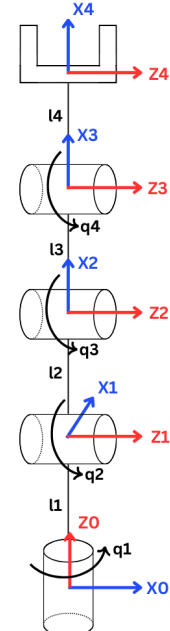


Fig. 4: Frame Assignment for DH Convention

Then the DH parameters table was constructed as shown in Table II. Where (θ_i) and (d_i) represent the rotation and translation along the (Z_{i-1}) axis respectively while (α_i) and (a_i) represent the rotation and translation along the (X_i) axis respectively.

TABLE II: DH Parameters

Joint _i	θ_i	d_i	α_i	a_i
1	q_1	l_1	0	$\frac{\pi}{2}$
2	q_2	0	l_2	0
3	q_3	0	l_3	0
4	q_4	0	l_4	0

The general form for the Transformation Matrix of frame (i) in respect with frame (i-1) is shown in Equation 1.

$${}^{i-1}T_i = \begin{bmatrix} C\theta_i & -S\theta_i C\alpha_i & S\theta_i S\alpha_i & a_i C\theta_i \\ S\theta_i & C\theta_i C\alpha_i & -C\theta_i S\alpha_i & a_i S\theta_i \\ 0 & S\alpha_i & C\alpha_i & d_i \\ 0 & 0 & 0 & 1 \end{bmatrix} \quad (1)$$

The four transformation matrices are as follows

$${}^0T_1 = \begin{bmatrix} Cq_1 & 0 & Sq_1 & 0 \\ Sq_1 & 0 & -Cq_1 & 0 \\ 0 & 1 & 0 & l_1 \\ 0 & 0 & 0 & 1 \end{bmatrix} \quad (2)$$

$${}^1T_2 = \begin{bmatrix} Cq_2 & -Sq_2 & 0 & l_2 Cq_2 \\ Sq_2 & Cq_2 & 0 & l_2 Sq_2 \\ 0 & 0 & 1 & 0 \\ 0 & 0 & 0 & 1 \end{bmatrix} \quad (3)$$

$${}^2T_3 = \begin{bmatrix} Cq_3 & -Sq_3 & 0 & l_3 Cq_3 \\ Sq_3 & Cq_3 & 0 & l_3 Sq_3 \\ 0 & 0 & 1 & 0 \\ 0 & 0 & 0 & 1 \end{bmatrix} \quad (4)$$

$${}^3T_4 = \begin{bmatrix} Cq_4 & -Sq_4 & 0 & l_4 Cq_4 \\ Sq_4 & Cq_4 & 0 & l_4 Sq_4 \\ 0 & 0 & 1 & 0 \\ 0 & 0 & 0 & 1 \end{bmatrix} \quad (5)$$

The total homogenous transformation matrix is as follows

$${}^0T_4 = {}^0T_1 \cdot {}^1T_2 \cdot {}^2T_3 \cdot {}^3T_4 \quad (6)$$

VII. SIMSCAPE SIMULATIONS

This section contains the simscape model of the robot, the 3D viewer of the robot using Simscape's Mechanics Explorer, and the results of two cases on input angles where the robot position from Simscape is compared to that of the DH convention. First, the Simscape model of the robot can be seen in Figure 5. Additionally, the 3D view of the robot on Mechanics Explorer can be observed in Figure 6. The angle q_1 is responsible for the base link's rotation, the angle q_2 is responsible for link 1's rotation, the angle q_3 is responsible for link 2's rotation and finally, the angle q_4 is responsible for the gripper's rotation.

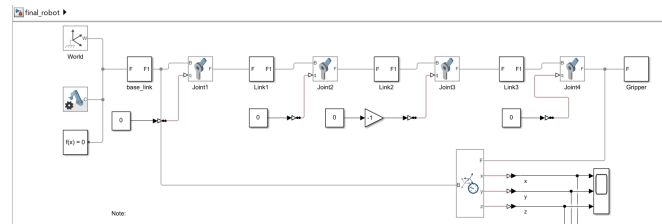


Fig. 5: Simscape Model of the Robot



Fig. 6: 3D view of the robot on Simscape

Two cases are used to simulate the robot and ensure correctness between the DH convention equations and the simscape end effector position. The first case is the equilibrium position where the robot is standing vertically upward and the joint angles are all equal to 0. The values obtained from the MATLAB code and Simscape simulations are seen in Figures 7 and 8. It is apparent that they are approximately equal within a small tolerance due to dimensions not taken into account in the DH convention such as the small depth values between the links. Finally, the robot's position in 3D is readily seen in Figure 9.

```
X =
1.6778e-14
Y =
0.2182
Z =
317.5499
```

Fig. 7: Case 1 MATLAB Results

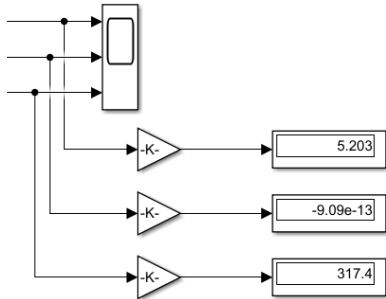


Fig. 8: Case 1 Simscape Results



Fig. 9: Case 1 Robot Position

The second case is a more general case where:

$$q_1 = 0.5 \text{ rad} \quad (7)$$

$$q_2 = 0.4 \text{ rad} \quad (8)$$

$$q_3 = 0.5 \text{ rad} \quad (9)$$

$$q_4 = 0 \text{ rad} \quad (10)$$

The values obtained from the MATLAB code and Simscape simulations are seen in Figures 10 and 11. Since the joint q_1 is actuated, the robot has a position on the Y-axis as if q_1 was not actuated, then the joints q_2 and q_3 would simply move the robot in the Z-X plane. Note that q_1 is a rotation around a vertical axis and q_2 and q_3 are rotations around axes out of the page. Finally, q_4 is the rotation of the gripper also around an axis out of the page. It is apparent that they are approximately equal within a small tolerance due to dimensions not taken into account in the DH convention such as the small depth values between the links. Finally, the robot's position in 3D is readily seen in Figure 12.

X =	-140.0417
Y =	-76.3126
Z =	255.7942

Fig. 10: Case 2 MATLAB Results

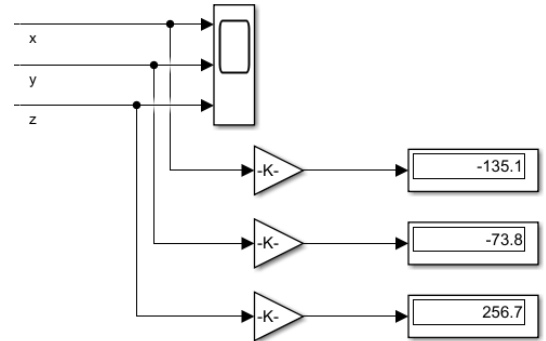


Fig. 11: Case 2 Simscape Results



Fig. 12: Case 2 Robot Position

The constraints of the system are represented as below. Only the base link's angle q_1 can rotate through 360° while the others are restricted to 90° to avoid extreme positions.

$$q_1 \in [0, 2\pi] \text{ rad} \quad (11)$$

$$q_2 \in [0, \frac{\pi}{2}] \text{ rad} \quad (12)$$

$$q_3 \in [0, \frac{\pi}{2}] \text{ rad} \quad (13)$$

$$q_4 \in [0, \frac{\pi}{2}] \text{ rad} \quad (14)$$

VIII. COPPELIASIM SIMULATIONS

This section contains the CoppeliSim simulation of the robot and the results of two cases on input angles where the robot position from CoppeliSim is compared to that of the DH convention. First, the Simscape model of the robot can be seen in Figure 13.

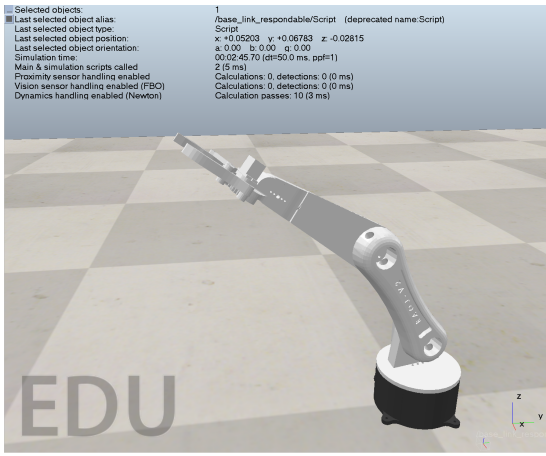


Fig. 13: CoppeliaSim Robot Simulation

Two cases are used to simulate the robot and ensure correctness between the DH convention equations and the CoppeliaSim end effector position. The first case is the equilibrium position where the robot is standing vertically upward and the joint angles are all equal to 0. The values obtained from the python code and CoppeliaSim simulations are seen in Figures 14 and 15. It is apparent that they are approximately equal within a small tolerance due to dimensions not taken into account in the DH convention such as the small depth values between the links.

```
PS C:\Users\youss\Desktop\Optimization> & C:/Users/youss/AppData/L
Gripper Position: [1.67776611e-17 1.67776611e-17 3.18000000e-01]
```

Fig. 14: Case 1 Python Results

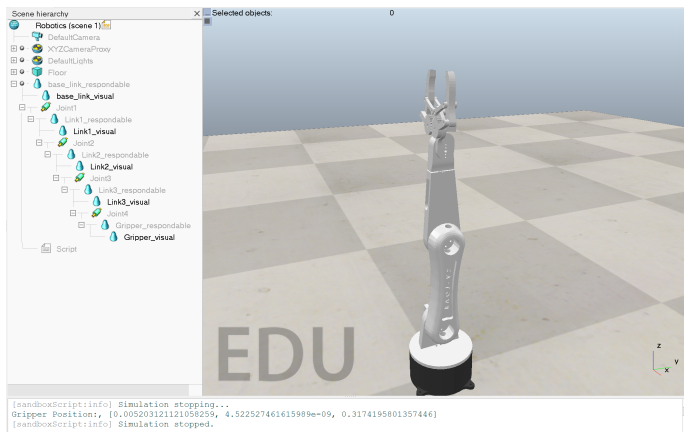


Fig. 15: Case 1 CoppeliaSim Results

The second case is a more general case where:

$$q_1 = 0.5 \text{ rad} \quad (15)$$

$$q_2 = 0.4 \text{ rad} \quad (16)$$

$$q_3 = 0.5 \text{ rad} \quad (17)$$

$$q_4 = 0 \text{ rad} \quad (18)$$

The values obtained from the MATLAB code and Simscape simulations are seen in Figures 16 and 17. It is apparent that they are approximately equal within a small tolerance due to dimensions not taken into account in the DH convention such as the small depth values between the links.

```
PS C:\Users\youss\Desktop\Optimization> & C:/Users/youss/
Gripper Position: [-0.13996071 -0.07646088 0.25624427]
```

Fig. 16: Case 2 Python Results

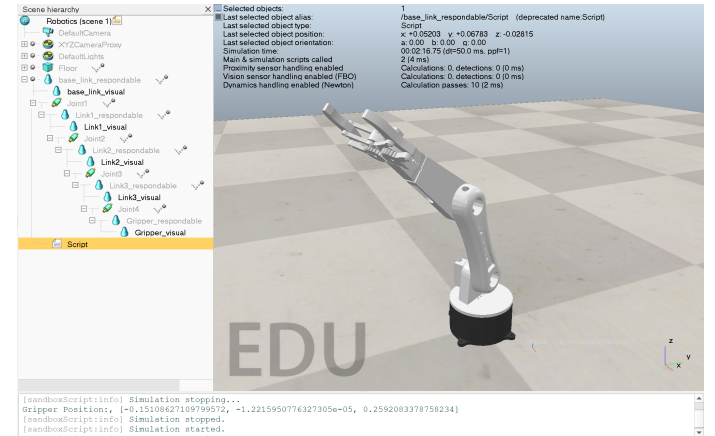


Fig. 17: Case 2 CoppeliaSim Results

The constraints of the system are represented as below. Only the base link's angle q_1 can rotate through 360° while the others are restricted to 90° to avoid extreme positions.

$$q_1 \in 0, 2\pi \text{ rad} \quad (19)$$

$$q_2 \in 0, \frac{\pi}{2} \text{ rad} \quad (20)$$

$$q_3 \in 0, \frac{\pi}{2} \text{ rad} \quad (21)$$

$$q_4 \in 0, \frac{\pi}{2} \text{ rad} \quad (22)$$

IX. HARDWARE ASSEMBLY

This section shows the hardware assembly process.



(a) Gripper Front View



(b) Gripper Back View

Fig. 18: Gripper Fabrication



(a) Robot with Gripper Assembled



(b) Fabricated Gripper with Link

Fig. 19: Robot Links



Fig. 20: Robot Assembled with Links without Gripper

REFERENCES

- [1] L. Antão, R. Pinto, J. Reis, G. Gonçalves, and F. L. Pereira, “Cooperative human-machine interaction in industrial environments,” in *2018 13th APCA International Conference on Automatic Control and Soft Computing (CONTROLO)*, pp. 430–435, IEEE, 2018.
- [2] A. Olivares-Alarcos, S. Foix, and G. Alenyà, “On inferring intentions in shared tasks for industrial collaborative robots,” *Electronics*, vol. 8, no. 11, p. 1306, 2019.
- [3] J. C.-Y. Ngu, C. C.-W. Lin, C. J.-Y. Sia, and N.-Z. Teo, “A narrative review of the medtronic hugo ras and technical comparison with the intuitive da vinci robotic surgical system,” *Journal of Robotic Surgery*, vol. 18, no. 1, p. 99, 2024.
- [4] I. F. Zidane, Y. Khattab, S. Rezeka, and M. El-Habrouk, “Robotics in laparoscopic surgery-a review,” *Robotica*, vol. 41, no. 1, pp. 126–173, 2023.
- [5] C. Lytridis, C. Bazinas, I. Kalathas, G. Siavalas, C. Tsakmakis, T. Spirlantis, E. Badeka, T. Pachidis, and V. G. Kaburlasos, “Cooperative grape harvesting using heterogeneous autonomous robots,” *Robotics*, vol. 12, no. 6, p. 147, 2023.
- [6] C. Lytridis, V. G. Kaburlasos, T. Pachidis, M. Manios, E. Vrochidou, T. Kalampokas, and S. Chatzistamatis, “An overview of cooperative robotics in agriculture,” *Agronomy*, vol. 11, no. 9, p. 1818, 2021.
- [7] C. Morar, I.-A. Doroftei, I. Doroftei, and M. Hagan, “Robotic applications on agricultural industry. a review,” in *IOP Conference Series: Materials Science and Engineering*, vol. 997, p. 012081, IOP Publishing, 2020.
- [8] A. Yeshmukhametov, K. Koganezawa, Z. Buribayev, Y. Amirgaliyev, and Y. Yamamoto, “Development of continuum robot arm and gripper for harvesting cherry tomatoes,” *Preprints*, 2019. Available online: <https://www.preprints.org/manuscript/201910.0162.v1>.
- [9] A. Dzedzickis, J. Subačiūtė-Žemaitienė, E. Šutinys, U. Samukaitė-Bubnienė, and V. Bučinskas, “Advanced applications of industrial robotics: New trends and possibilities,” *Applied Sciences*, vol. 12, no. 1, 2022.
- [10] B. Kokane Sanket, S. Kalamurkar Shalaka, and B. Khose Suyog, “Robotics in food processing industries: A review,” *The Pharma Innovation Journal*, vol. 11, no. 7S, pp. 948–953, 2022.
- [11] J. Wan, S. Tang, Q. Hua, D. Li, C. Liu, and J. Lloret, “Context-aware cloud robotics for material handling in cognitive industrial internet of things,” *IEEE Internet of Things Journal*, vol. 5, no. 4, pp. 2272–2281, 2017.
- [12] P. Segura, O. Lobato-Calleros, A. Ramírez-Serrano, and I. Soria, “Human-robot collaborative systems: Structural components for current manufacturing applications,” *Advances in Industrial and Manufacturing Engineering*, vol. 3, p. 100060, 2021.
- [13] M. Blatnický, J. Dižo, J. Gerlici, M. Sága, T. Lack, and E. Kuba, “Design of a robotic manipulator for handling products of automotive industry,” *International Journal of Advanced Robotic Systems*, vol. 17, no. 1, p. 1729881420906290, 2020.